Radiolabeled bombesin analogs for prostate cancer diagnosis: preclinical studies

Bluma Linkowski Faintuch[a,*], Rodrigo Teodoro[a], Adriano Duatti[b],
Emiko Muramoto[a], Salomao Faintuch[c], Charles J. Smith[d]

[a]Radiopharmacy Center, Institute of Energetic and Nuclear Research, Sao Paulo, SP 05508-000, Brazil
[b]Laboratory of Nuclear Medicine, Department of Clinical and Experimental Medicine, University of Ferrara, Ferrara, 44100, Italy
[c]Department of Radiology, Beth Israel Deaconess Medical Center, Boston, MA 02215, USA
[d]Department of Radiology, Missouri University Research Reactor, and Radiopharmaceutical Sciences Institute,
University of Missouri-Columbia, The Harry S. Truman Memorial Veterans' Hospital, Columbia, MO 65201, USA

Abstract

Introduction: Radionuclide imaging can be a useful tool for the diagnosis of prostate cancer. Bombesin (BBN) is a molecule with high affinity for gastrin releasing peptide (GRP) receptors which are over-expressed in that tumor. This report compares ^{99m}Tc-HYNIC-βAla-BBN (7-14)NH2 [^{99m}Tc-HYNIC-BBN] and ^{99m}Tc≡N(PNP6)-Cys-βAla-BBN(7-14)NH2 [^{99m}TcN(PNP6)-Cys-BBN] with regard to labeling procedures as well as in vitro and in vivo evaluation (biodistribution and scintigraphic imaging).
Methods: Peptide synthesis was performed in an automated peptide synthesizer. HYNIC-BBN was radiolabeled with pertechnetate using tricine and ethylenediamine diacetic acid (EDDA) as coligands. Cys- BBN was radiolabeled in a two-step procedure with the preparation of the precursor ^{99m}Tc-Nitrido first and then introducing diphosphine (PNP6). Radiochemical evaluation of conjugates, as well as studies of stability, transchelation toward cysteine, and partition coefficient were done. Biological studies included internalization, biodistribution in healthy animals and in animals bearing PC3 cancer cells with acquisition of images from the tumor-bearing animals.
Results: Both complexes showed a high radiochemical yield along with good stability. Biodistribution studies pointed out strong renal excretion for the former complex due to its hydrophilic profile and marked hepatobiliary excretion for the latter, corresponding to observed lipophilicity. Tumor uptake was higher for ^{99m}Tc-HYNIC-BBN and the same occurred with internalization findings, which exceeded those of ^{99m}TcN(PNP6)-BBN. Blocking studies in mice bearing PC-3 tumor cells revealed significantly reduced pancreas and tumor uptake, demonstrating receptor specificity of the conjugates.
Conclusion: The best radiotracer was ^{99m}Tc-HYNIC-BBN on the basis of high radiochemical yield, fast radiolabeling procedure without need for a purification step, and more consistent tumor uptake.
© 2008 Elsevier Inc. All rights reserved.

Keywords: Bombesin analogs; technetium 99m (^{99m}Tc)-HYNIC-BBN; Prostate cancer; ^{99m}TcN(PNP6)-Cys-BBN

1. Introduction

Small receptor-binding peptides are currently the agents of choice for receptor imaging and tumor targeting. Several malignant tumors overexpress cell surface receptors, which can be targeted with radiolabeled receptor-specific peptides for imaging and therapy [1].

Bombesin (BBN), first isolated from frog skin, is a 14-amino-acid neuropeptide with high affinity for gastrin-releasing peptide (GRP) receptors [2,3]. BBN and its mammalian counterpart GRP, which is a 27-amino-acid peptide, have similar biological properties and share a nearly identical C-terminal amino acid sequence. GRP may function as a paracrine/autocrine growth stimulator in many neoplasms [4–6].

Four subtypes of BBN/GRP receptors have been identified. The first two to be cloned were designated BB1

and BB2 and were originally referred to as the neuromedin B- and GRP-preferring bombesin receptors after their respective endogenous ligands. More recently, a third mammalian bombesin receptor subtype, BB3, was cloned, although no endogenous ligand has been identified to date. A fourth bombesin receptor, BB4, has been cloned from the frog, but as yet, there is only a partial sequence for the mammalian equivalent [7]. Specific receptors for BBN are overexpressed on a variety of human tumors, including small cell lung cancer, prostate, breast, gastric, colon and pancreatic cancers as well as gliobastoma [7]. Radiolabeled BBN analogs having high affinity for these receptors might therefore be used for scintigraphic imaging of those tumor types [4,8].

BBN analogs with high stability and potency in vivo have been developed and evaluated [9]. Several of these analogs bind selectively and avidly to GRP receptors on cancer cells, both in vitro and in vivo, using BBN (1–14) full-length sequence or the truncated amino acid sequence comprising the GRP-receptor binding moiety as BBN(7-14)NH$_2$. It has been shown that the C-terminal amino acid sequence BBN (7-14)NH$_2$ is necessary for retaining receptor binding affinity and preserving the biological activity of BBN-like peptide [10]. Hence, the N-terminal region of the peptide can be used for radiolabeling.

Efforts have been made to design derivatized BBN analogs. Because BBN agonists are generally preferable to BBN antagonists for receptor-specific internalization, most BBN analogs with an amidated C-terminus are directly involved in the specific binding interaction with the gastrin releasing peptide receptor [11]. Design has also focused on such features as nature of the chelate, spacer group and introduction of other amino acids, all of which may influence GRP receptor binding affinity and residualization of radio-activity in cancer cells, thus improving the pharmacokinetics of the BBN conjugate [4–6].

The advent of novel technetium (Tc) cores upon which new radiopharmaceuticals could be based [i.e., Tc(I), reducible Tc(III), nonreducible Tc(III) and Tc(V)-nitrido] have expanded the potential uses of Tc in diagnostic nuclear medicine [12]. Bifunctional chelating agents such as MAG$_3$, N$_2$S$_2$, tripeptide triamino-thiol (N$_3$S), S$_4$, P$_2$S$_2$, DTPA, 2-picolylamine-*N,N*-diacetate and the *N*α-histidinyl acetate-carbonyl have been used for stabilization of the radioactive metal center under in vivo conditions [13]. Some examples are ^{99m}Tc-RP-527 [14,15] that contains a N$_3$S chelating moiety, ^{99m}Tc-Demobesin 1 with a novel tetraamine (N4) derivatized BBN analog [16] and ^{99m}Tc-P$_2$S$_2$-BN(7-14) [17] that uses a phosphine chelating system for preconjugation approach.

Methods for preparation of ^{99m}Tc-radiopharmaceuticals containing the Tc≡N multiple bond was proposed by Baldas and Bonnyman [18] in 1985. However, not until 1990 did Pasqualini's group [19] develop a method to combine biologically active molecules with stable ^{99m}Tc-nitrido complexes. The incorporation of a bioactive molecule into a nitrido-containing ^{99m}Tc complex has been successfully achieved by using the [^{99m}TcN(PNP)]$^{2+}$ metal fragment [20].

The molecular structure of the five-coordinate, nitrido ^{99m}Tc complexes fall essentially into two main categories — symmetrical and asymmetrical. A symmetrical ^{99m}Tc nitrido complex is formed when a ^{99m}Tc≡N group is coordinated by two identical bidentate ligands. Asymmetrical complexes possess a distorted trigonal bipyramidal structure in which 2 different bidentate ligands are bound to the same [^{99m}Tc≡N]$^{+2}$ core [20]. The [^{99m}Tc≡N]$^{2+}$ core constitutes a group isoelectronic with [^{99m}Tc=O]$^{3+}$ and [O=^{99m}Tc=O]$^+$.

The nitrido N^{3-} ligand is considered to be the strongest π donor and may act as a terminal or bridging atom which stabilizes the metal in high oxidation states [21]. Therefore, biologically active targets containing the ^{99m}Tc-nitrido core have some propensity for development of in vivo stable conjugates for diagnosis of specific human cancers.

2-Hydrazinonicotinamide (HYNIC) is a bifunctional chelating ligand that has received considerable interest in recent years toward design and development of Tc- and rhenium-based radiopharmaceuticals. Zinn et al. [22] investigated the adenoviral gene transfer of GRP using a ^{99m}Tc-HYNIC-BBN conjugate. Radiolabeling studies of ^{99m}Tc-HYNIC-BBN were previously published by our group [6], and additional articles about the use of the ^{99m}Tc-nitride core with BBN analogs could not be found in the literature.

We herein report a detailed comparative study between ^{99m}Tc-HYNIC-BBN and ^{99m}TcN(PNP6)-Cys-BBN that includes synthesis, radiolabeling and in vitro and in vivo evaluation of the two conjugates.

2. Materials and methods

The investigation was conducted at the Radiopharmacy Center, Institute of Energetic and Nuclear Research/Brazilian Commission of Nuclear Energy (IPEN/CNEN), Sao Paulo, Brazil, in collaboration with the Harry S. Truman Memorial Veterans Hospital, Columbia, MO, USA, and the University of Ferrara, Italy. All animal studies were performed at the Radiopharmacy Center, IPEN/CNEN, and the protocol was approved by the local animal welfare committee.

- ^{99m}Tc was obtained from an alumina-based ^{99}Mo/^{99m}Tc generator, supplied by the Radiopharmacy Center of the Institute of Energetic and Nuclear Research (IPEN/CNEN).
- The nitrido kit was supplied by Schering CIS Bio International, and bis(diethoxipropylphosphinoethyl) ethoxy ethylamine (PNP6) was prepared at the University of Ferrara, Italy.
- 6-BOC-hydrazinonicotinic acid was purchased from SoluLink Biosciences, San Diego, CA, USA.
- All other reagents such as tricine, ethylenediamine-*N*, *N*′-diacetic acid (EDDA) and SnCl$_2$.2H$_2$O were purchased from Sigma–Aldrich (Sao Paulo, Brazil).

- Swiss mice and nude mice for imaging and biodistribution studies were provided by the Animal Facility of IPEN-CNEN.

2.1. Peptide synthesis

HYNIC-BBN and Cys-BBN were prepared as previously reported [6] at The Harry S. Truman Memorial Veterans Hospital on a Perkin-Elmer Applied Biosystem Model 432 automated solid phase peptide synthesizer (SPSS) employing traditional Fmoc chemistry. Crude peptide conjugates were purified by semipreparative high-performance liquid chromatography (HPLC) and fully characterized by electrospray ionization–mass spectrometry (ESI-MS).

2.2. Radiolabeling of HYNIC-BBN with pertechnetate

To a sealed reaction vial containing 20 mg tricine and 5 mg of EDDA was added 0.5 ml of 0.1 M nitrogenated phosphate-buffered solution (PBS). Ten micrograms of HYNIC-BBN, 5 µl of 8.9 mM $SnCl_2.2H_2O$ solution in 0.1 N HCl (nitrogen-purged) and 500 µl of $Na^{99m}TcO_4$ was added to the PBS. The solution was heated for 15 min in a water bath at 100°C and cooled to room temperature. The pH of the reaction mixture was 7.

2.3. Radiolabeling of Cys-BBN with ^{99m}Tc-nitrido precursor

Radiolabeling of Cys-BBN was conducted via a two-step procedure. The ^{99m}Tc-nitrido precursor species was synthesized as follows: To a readily-available lyophilized kit (Schering CIS Bio International) containing succinic acid dihydrazide (SDH), nitrido-donor ligand and stannous chloride reduction agent were added 0.5 ml of aqueous $Na^{99m}TcO_4$ and 0.5 ml of absolute ethanol. The reaction vial was left standing at room temperature for a period of 30 min. $^{99m}TcN(PNP6)$-Cys-BBN was prepared by addition of 50 µl of a 0.9 mM aqueous solution of Cys-BBN and 3 µg of diphosphine (PNP6) (dissolved in 200 µl of ethanol) to the precursor solution vial. This reaction mixture was incubated for 1 h at 100°C.

2.4. Radiochemical evaluation of ^{99m}Tc-HYNIC-BBN conjugate and $^{99m}Tc(N)(PNP6)$-Cys-BBN

Radiochemical analysis of the ^{99m}Tc-HYNIC-BBN conjugates was performed by instant thin-layer chromatography (ITLC) on silica gel strips (ITLC-SG, Gelman Sciences, Ann Arbor, MI, USA) using a 2-solvent system, namely, methylethylketone (MEK) for detection of $^{99m}TcO_4^-$ and 50% acetonitrile (ACN) for $^{99m}TcO_2$.

Radiochemical evaluation of the Tc≡N kit and $^{99m}Tc(N)$(PNP6)-Cys-BBN was performed using ITLC-SG with a solvent system ethanol/chloroform/toluene/ammonium acetate 0.5 M (E/C/T/AA, 5; 3; 3; 0.5). Ethyl acetate was employed to detect $^{99m}TcO_4^-$ and ^{99m}TcN, along with ethanol/water (1:1) for $^{99m}TcO_2$.

Both radiolabeled conjugates were also characterized by reverse-phase HPLC (RP-HPLC). This analysis was performed on a Waters 600E system equipped with a Waters 486 tunable absorbance detector, an in-line Packard 150TR flow scintillation analyzer and a Waters 746 data module. HPLC solvents consisted of H_2O containing 0.1% trifluoroacetic acid (Solvent A) and ACN containing 0.1% trifluoracetic acid (Solvent B). A Symmetry C-18 column (5.0 µm, 100 Å, 4.6×250 mm, Waters, Milford, MA, USA) was used with a flow rate of 0.5 ml/min. The HPLC gradient system began with a solvent composition of 95% A and 5% B and followed a linear gradient of 30% A:70% B from 0 to 25 min and 30% A:70% B to 5% A:95% B from 25 to 30 min.

2.5. Purification of the radiolabeled conjugates

Purification was conducted only for $^{99m}TcN(PNP6)$-Cys-BBN because radiochemical purity achieved with ^{99m}Tc-HYNIC-BBN was sufficiently high for in vitro and in vivo studies. The purification was executed by use of a C_{18}-SepPak-Mini cartridge (Waters). The column was activated with 5 ml of ethanol and 5 ml of water. The impurities were eluted with 2 ml of water, and the radiolabeled peptide, with 2 ml of ethanol. For biological studies and other evaluations, the ethanol solvent was slowly evaporated under a nitrogen atmosphere. Isotonic saline was used for dissolution of conjugates prior to in vitro and in vivo applications.

2.6. Radiochemical stability, transchelation toward cysteine and partition coefficient

^{99m}Tc-HYNIC-BBN and $^{99m}TcN(PNP6)$-Cys-BBN radiochemical stability was observed over a time period of 6 h at room temperature. Transchelation of the new conjugates to cysteine (0.01–100 mM) was also studied at 1, 2 and 4 h at 37°C. Partition coefficients for each conjugate were also evaluated in octanol/H_2O. The partition ratios of the labels were calculated by dividing the counts in the organic phase with those in the aqueous phase per volume unit.

2.7. Cell culture

Human androgen-independent prostate carcinoma PC3 cells were grown in Dulbecco's MEM GLUTAMAX-I supplemented by 10% (v/v) fetal bovine serum, 100 U/ml penicillin and 100 µg/ml streptomycin. Cells were kept in humidified air containing 5% CO_2 at 37°C. The cells were grown to confluency and then harvested by trypsinization. After centrifugation (5 min at 100g), cells were resuspended in PBS, counted, centrifuged once again and resuspended in PBS (70 µl) for inoculation into animals.

2.8. Inoculation of PC3 cells in nude mice

Athymic male nude mice (18–22 g) were injected subcutaneously on the upper part of the back with a suspension containing $5.0×10^6$ cells. PC3 cells were allowed to grow in vivo 2–3 weeks post inoculation, thus forming tumors with a diameter of 1cm approximately.

Tumor-bearing mice were used in the biodistribution and imaging studies.

2.9. Internalization studies

Internalization of the two radiotracers was analyzed using confluent PC3 cells in six-well plates in triplicate (1.10^6 cells/well). They were incubated with the radiotracers with and without excess of 1 μM cold HYNIC-BBN or cold 1 μM Cys-BBN, for periods of 30 min and 2 h at 37°C, in triplicates for each time point, for nonspecific internalization.

After this step, the supernatant was collected and cell surface-bound radioligand was removed by acid wash buffer (50 mM glycine buffer pH 2.8, 0.1 M NaCl) at room temperature for 5 min. Internalized radioligand was determined by solubilization of the cells with 1 N NaOH. Results were expressed as percentage of total radioactivity, considering cell surface bound activity plus internalized activity.

2.10. Biodistribution experiments in healthy Swiss mice and in nude mice bearing PC3 tumor cells

Upon purification, ^{99m}Tc-labeled preparations (185-370 MBq/ml, 0.1 ml) were administrated into the tail vein in healthy male Swiss mice (body mass 20–25 g) and in nude mice (body mass 18–22 g) bearing PC3 tumors.

Healthy mice were sacrificed in groups of 6 at 1.5 and 4 h post injection. Tumor-bearing mice were sacrificed in groups of 6 at 1.5 h post injection. Organs and tissues (blood, heart, lung, spleen, kidneys, liver, pancreas, stomach, large and small intestine, muscle, bone) were excised and weighed and the radioactivity was determined by γ-counting. Results were expressed as percentage of injected dose per gram (%ID/g) of tissue. Receptor blocking studies were also carried out by administration of 100 μg of cold BBN along with the radiopeptide.

2.11. Tumor imaging

Anesthetized mice were horizontally placed under the collimator of a Mediso Imaging System, Budapest, Hungria, employing an low-energy high-resolution collimator. Images
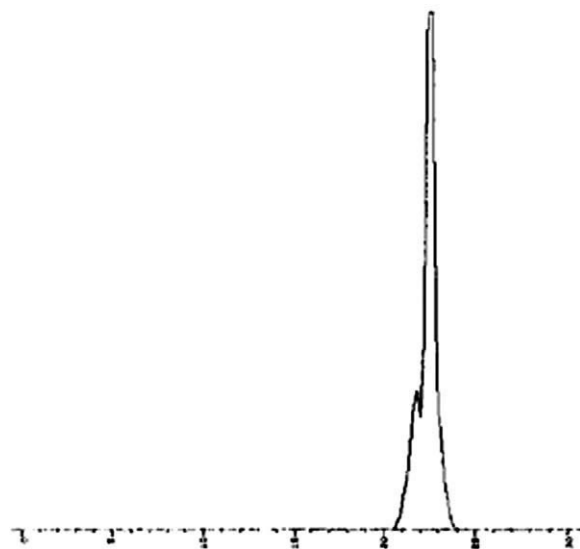

Fig. 2. HPLC profile of ^{99m}TcN(PNP6)-Cys-BBN.

were acquired at 1.5 h post injection using a 256×256×16 matrix size with a 20% energy window set at 140 keV for a period of 180 s.

3. Results

3.1. Synthesis of peptide conjugates

The BBN(7-14)NH$_2$ peptide conjugates were conveniently synthesized by SPPS. The yields of the HPLC purified conjugates were approximately 50%. ESI-MS analyses were consistent with the molecular weights calculated for each conjugate.

3.2. Radiolabeling of HYNIC-BBN with pertechnetate

Radiochemical purity of ^{99m}Tc-HYNIC-BBN conjugate was evaluated by ITLC using a solvent system of MEK and 50% ACN solution. In MEK, ^{99m}TcO$_4^-$ had an R_f of 1, whereas for ^{99m}TcO$_2$ and the radiolabeled conjugate the R_f was 0. In ACN solution, ^{99m}TcO$_4^-$ and the radiolabeled conjugate displayed an R_f of 1 and ^{99m}TcO$_2$ an R_f of 0.
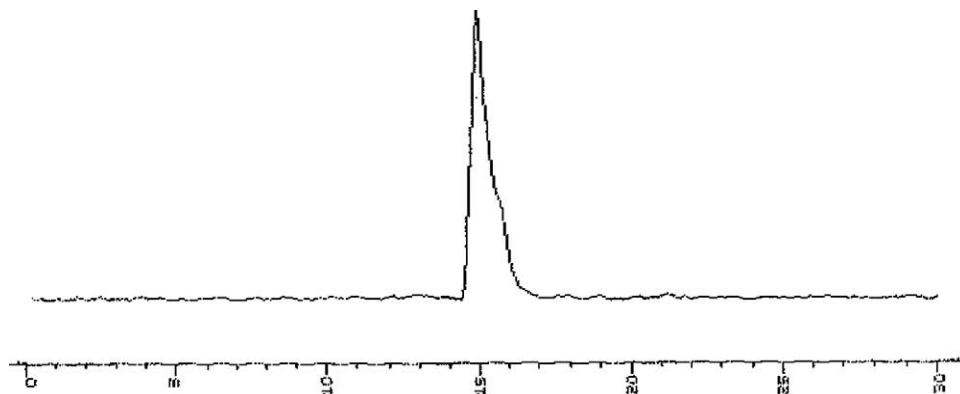

Fig. 1. HPLC profile of ^{99m}Tc-HYNIC-BBN.

Radiochemical yield obtained for the exchange radiolabeling system, ^{99m}Tc-HYNIC-BBN+tricine+EDDA was ≥99%. The chromatograms show a single peak for ^{99m}Tc-HYNIC-BBN and conjugate, with a retention time of 15.2 min. Pertechnetate had a retention time of 5.3 min under these HPLC conditions (Fig. 1).

3.3. Radiolabeling of Cys-BBN with ^{99m}Tc-nitrido precursor

Radiochemical yield for the ^{99m}Tc≡N precursor was 97.5±1.1%. Radiochemical purity for the ^{99m}TcN(PNP6)-Cys-BBN conjugate was 96.3±1.3%. Thin layer chromatography (TLC) analysis with a solvent composition of E/C/T/A allowed for determination of Tc≡N precursor and ^{99m}TcO$_4^-$. The R_f values for these two species was 0–0.1 and 0.9–1.0, respectively. To check for the presence of ^{99m}TcO$_2$, ethanol/water was used. In this solvent mixture, Tc≡N migrates to the solvent front. One major species was observed in the HPLC chromatographic profile at 22.8 min. A small shoulder at 22.0 min indicates the presence of a metallated conjugate with similar chromatographic properties to the major product (Fig. 2).

3.4. Radiochemical stability, transchelation toward cysteine and partition coefficient

Radiochemical stability was evaluated for both radiopharmaceuticals at time-points of 1, 2, 4 and 6h. It was observed that both species exhibited excellent radiochemical stability even for extended periods of time. ^{99m}Tc-HYNIC-BBN had 100% of stability at 6 h. ^{99m}TcN(PNP6)-Cys-BBN, on the other hand, did exhibit some dissociation with loss of conjugate being ~2.3%.

The radiopharmaceuticals were also challenged with excess cysteine to determine their stability against ligand exchange and/or decomposition. The samples were analyzed by means of ITLC at 1, 2 and 4 h. Findings confirmed that the radiolabeled peptides are quite inert regarding transchelation by free cysteine (Table 1). For the radiolabeled HYNIC conjugate, the change was −1.4% and for the radiolabeled nitrido conjugate, −4.1% from blank (no cysteine) to 4 h with 100 mM of cysteine.

Partition coefficients of the radiolabeled peptides were determined by the ratio between *n*-octanol and water.

Table 1
Cysteine transchelation (%RP)

Cysteine (mM)/ product	1	2	1	2	1	2
	1 h		2 h		4 h	
0	99.7	97.7	99.7	95.9	99.7	95.4
0.01	97.0	97.5	97.9	93.9	98.3	94.5
0.1	98.9	97.5	98.4	94.6	98.5	94.4
1	99.2	97.2	98.3	94.6	98.4	94.2
10	99.6	95.3	98.4	94.4	98.7	94.1
50	99.7	96.1	98.3	94.5	98.7	93.0
100	99.6	95.1	98.4	94.6	98.3	93.6

1, ^{99m}Tc-HYNIC-BBN; 2, ^{99m}TcN(PNP6)-Cys-BBN.

Table 2
Internalization (%) of the radiotracers in PC3 cells

Time/radiotracers	^{99m}Tc-HYNIC-BBN	^{99m}TcN(PNP6)-Cys-BBN
30 min	12.1	8.9
2 h	18.5	15.5

The partition ratio of ^{99m}Tc-HYNIC-BBN was 0.02 (log P=−1.74) and, thus, within the hydrophilic range. However, ^{99m}TcN(PNP6)-Cys-BBN showed a partition coefficient of 9.51 (log P=0.98), demonstrating extreme lipophilic character.

3.5. Internalization results

Internalization measurements showed higher values for ^{99m}Tc-HYNIC–βAla-BBN with 12.1% and 18.5% internalized activity after 30 min and 2 h, respectively (Table 2). Internalization increased with time of incubation, as indicated.

3.6. Biodistribution experiments in healthy Swiss mice and in nude mice bearing PC3 tumor cells

Table 3 summarize the results of biodistribution studies in normal *Swiss* mice at 1.5 and 4 h post intravenous injection of ^{99m}Tc-HYNIC-BBN and ^{99m}TcN(PNP6)-Cys-BBN. The radiotracers had rapid blood clearance, with only 0.4 and 0.5%ID/ml for ^{99m}Tc-HYNIC-BBN and ^{99m}TcN(PNP6)-Cys-BBN, respectively, at 1.5 h, followed by further decrease at 4 h. The uptake of ^{99m}TcN(PNP6)-Cys-BBN by liver (9.1±1.0%ID/g), pancreas (4.8±0.2%ID/g) and intestine (15.7±2.4%ID/g) was expected considering the lipophilic character of the conjugate. Spleen and stomach showed minimal uptake of conjugate for both radiotracers. ^{99m}Tc-HYNIC-BBN showed some accumulation in kidney. For example, uptake was 8.4±2.8%ID/g in normal kidney at 1.5 h post injection. These studies affirmed that ^{99m}Tc-

Table 3
Biodistribution of ^{99m}Tc-HYNIC-BBN and ^{99m}TcN(PNP6)-Cys-BBN in healthy Swiss Mice

Tissue/ organ	^{99m}Tc-HYNIC-BBN		^{99m}TcN(PNP6)-Cys-BBN	
	1.5 h	4 h	1.5 h	4 h
Blood	0.40±0.16	0.28±0.11	0.47±0.01	0.25±0.07
Heart	0.18±0.06	0.09±0.02	0.37±0.14	0.18±0.01
Lung	0.42±0.18	0.19±0.08	0.69±0.28	0.33±0.01
Kidney	8.43±2.81	4.66±1.62	2.52±0.68	1.66±0.23
Liver	0.34±0.12	0.20±0.11	9.09±1.04	6.28±0.89
Spleen	0.22±0.09	0.13±0.05	0.68±0.15	0.53±0.06
Stomach	0.35±0.18	0.19±0.10	1.59±1.11	1.68±0.99
Pancreas	0.96±0.38	0.57±0.23	4.78±0.19	3.53±0.97
Intestine	1.43±0.31	0.72±0.08	15.70±2.41	25.51±2.95
Muscle	0.12±0.06	0.05±0.02	0.33±0.12	0.27±0.17
Bone	0.35±0.12	0.13±0.04	0.37±0.06	0.30±0.16

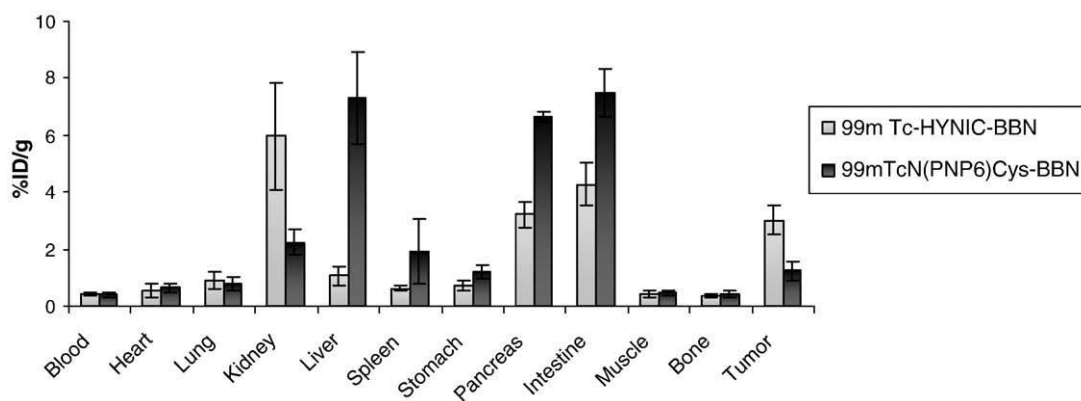Injected dose 0.1 ml/5.5 MBq. Data are expressed as percentage of %ID/g of tissue±S.D.

Fig. 3. Biodistribution studies of ^{99m}Tc-HYNIC-BBN and ^{99m}TcN(PNP6)-Cys-BBN in nude mice bearing PC3 tumor xenograft 1.5 h after injection.

HYNIC-BBN was excreted primarily by the renal-urinary system and primary elimination of ^{99m}TcN(PNP6)-Cys-BBN via the hepatobiliary system.

Radioactivity uptake for most tissues was lower in tumor-bearing mice than in healthy animals, especially in kidney. In contrast, pancreatic uptake of ^{99m}Tc-HYNIC-BBN in animals with cancer almost tripled in comparison to healthy animals, and the difference was two fold when ^{99m}TcN(PNP6) Cys-BBN was considered under the same circumstances. The highest tumor uptake was achieved when using the HYNIC conjugate: 3.0±0.5%ID/g vs. 1.2±0.3%ID/g for nitrido conjugate (Fig. 3).

Blocking studies in which 100 μg of cold HYNIC-BBN and cold Cys-BBN were coadministered to the ^{99m}Tc complexes reduced pancreas and tumor uptake significantly (Fig. 4, 5). The former conjugate blocked approximately 49% of tumor uptake, and for the last, 62% of tumor activity was suppressed (Table 4).

Concerning the pancreas, uptake diminished from 3.2± 0.5%ID/g to 0.7±0.1%ID/g and from 6.6±0.2%ID/g to 1.6± 0.2%ID/g for HYNIC and for nitrido tracers, respectively.

With ^{99m}TcN(PNP6)-Cys-BBN, uptake by the liver was also reduced in blocked animals, in contrast to increased uptake by lung, kidney and spleen (Fig. 5).

^{99m}Tc-HYNIC-BBN uptake decreased in lung, kidney, liver and intestine after blocking. Tumor/tissue ratio can be observed in Table 5. The best ratios were achieved with ^{99m}Tc-HYNIC-BBN, especially for tumor/blood and tumor/ muscle results. Nevertheless, all ratios were higher for this tracer when compared to ^{99m}TcN(PNP6)-Cys-BBN.

3.7. Tumor imaging

Scintigraphic studies performed in nude mice transplanted with prostate cancer cells demonstrated significant tumor uptake (Figs. 6 and 7). Blocking studies showed the specificity of the radiotracers. The region of interest (ROI) index of tumor for unblocked and blocked procedures using ^{99m}Tc-HYNIC-BBN was 4.4% and 1.5%, respectively (Fig. 6). For ^{99m}TcN(PNP6)-Cys-BBN (Fig. 7), it was 1.7% and 0.7%. The tumor was blocked in a range of 59–67%. Higher uptake of conjugate by the hepatobiliary excretory system was observed with ^{99m}TcN(PNP6)-Cys-BBN.

4. Discussion

Prostate cancer is the second leading cause of cancer death in American men. The American Cancer Society [23]
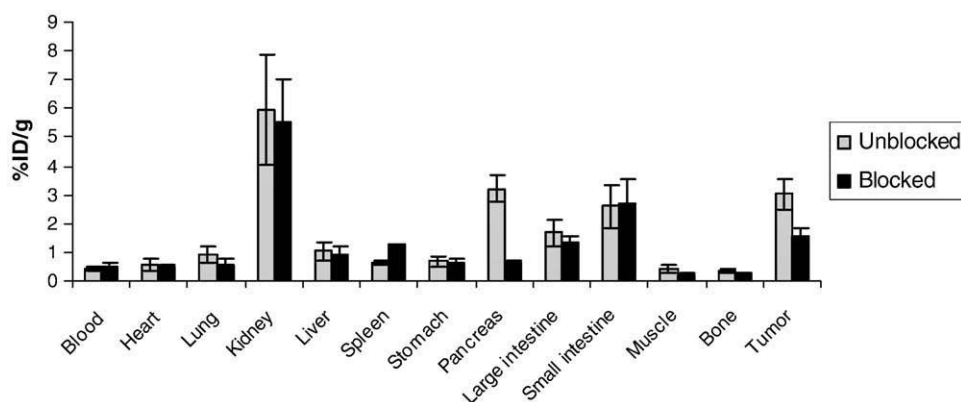

Fig. 4. Biodistribution studies of ^{99m}Tc-HYNIC-BBN in blocked and unblocked nude mice bearing PC3 tumor xenograft 1.5 h after injection.
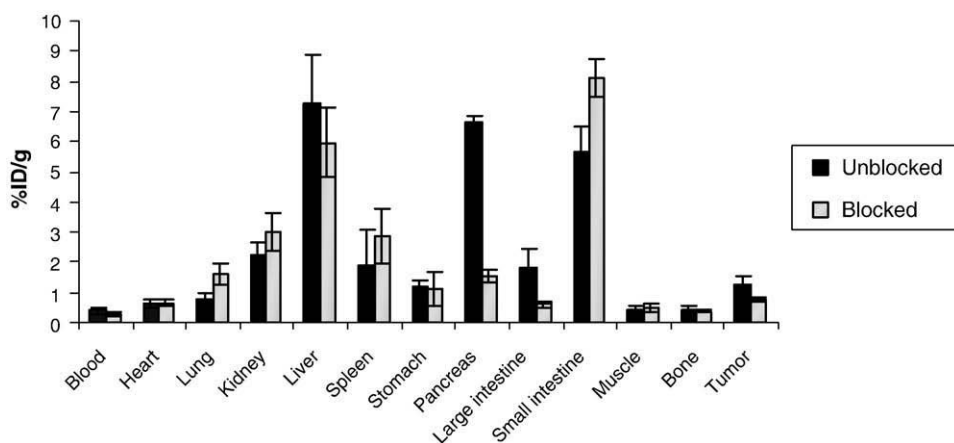
Fig. 5. Biodistribution studies of ^{99m}TcN(PNP6)-Cys-BBN in blocked and unblocked nude mice bearing PC3 tumor xenograft 1.5 h after injection.

estimates that during 2007 about 218,890 new cases of prostate cancer will be diagnosed in the United States and that 27,050 men will die from this disease. By the time they are first seen, 91% of all prostate cancers are confined to the prostate (local stage) or have spread to nearby areas (regional stage) but not to distant sites such as bone specific diagnostic tools that focus on pelvic anatomy would thus be particularly useful for screening and staging of the malignancy.

There is a theoretical pitfall for too early a diagnosis when slow-growing microscopic disease exists. Many of these patients are elderly and suffer from comorbidities. Therefore, certain cases might not require any treatment as they would probably die from other causes. However, clinical judgement permits relatively easy selection of those patients.

In the past, digital rectal examination was the first approach when the disease was suspected and biopsy of an eventual nodule would confirm the diagnosis. However, these procedures were not ideal for early diagnosis and did not permit tumor staging. The ability to localize an early event in prostate carcinogenesis with bombesin was reported by Markwalder and Reubi [24], who encountered massive gastrin-releasing peptide receptor overexpression not only in invasive prostate cancer but also in the prostatic intraepithelial neoplasia.

The synthesis and conjugation of HYNIC-βAla-BBN (7-14)NH$_2$ was described by Faintuch et al. [6], and Cys-βAla-BBN(7-14)NH$_2$ has also been conveniently synthesized by solid-phase peptide synthesis (Figs. 8 and 9).

For radiochemical evaluation of the new ^{99m}Tc-peptide conjugates, a combination of analytical methods (TLC and RP-HPLC) was used to assess each radiolabeling yield and radiochemical purity. The former is convenient for identification of [^{99m}Tc]colloid (^{99m}TcO$_2$) formation that is not available by HPLC. RP-HPLC is a powerful tool for separation of eventual mixtures including epimers and diastereo isomers [25].

Labeling of HYNIC-BBN with Tc-99m was performed in very high yield (>99%). The labeling protocol leads to the formation of a single radioactive species, as indicated by the HPLC chromatographic profile (Fig. 1). ^{99m}Tc binds to the hydrazine ligand forming a ^{99m}Tc≡N bond. HYNIC alone cannot satisfy the coordination requirements of Tc(V) because it can only occupy one or two coordination sites on the radionuclide. Coligands are necessary to complete the coordination sphere of the Tc (V) core. Several coligands have been developed to improve the ^{99m}Tc-radiolabeling of HYNIC-biomolecules [6]. The use of coligands allows for easy modification of the hydrophilicity and pharmacokinetics of ^{99m}Tc-labeled peptide conjugates. In the current labeling strategy, we opted for Tricine/EDDA exchange.

The radiochemical purity of ^{99m}TcN(PNP6)-Cys-BBN was very favorable (97.5±1.1%). However, it took more time to prepare and a purification step was required prior to *in vitro* and *in vivo* biological studies. The HPLC chromato-

Table 4
Uptake of radiopharmaceuticals in tumor site (%ID/g)

Uptake by the prostate tumor	^{99m}Tc-HYNIC-BBN	^{99m}TcN(PNP6)-Cys-BBN
Unblocked	3.0±0.5	1.2±0.3
Blocked	1.5±0.2	0.8±0.1

Table 5
Tumor-to-tissue ratio in nude mice bearing tumor

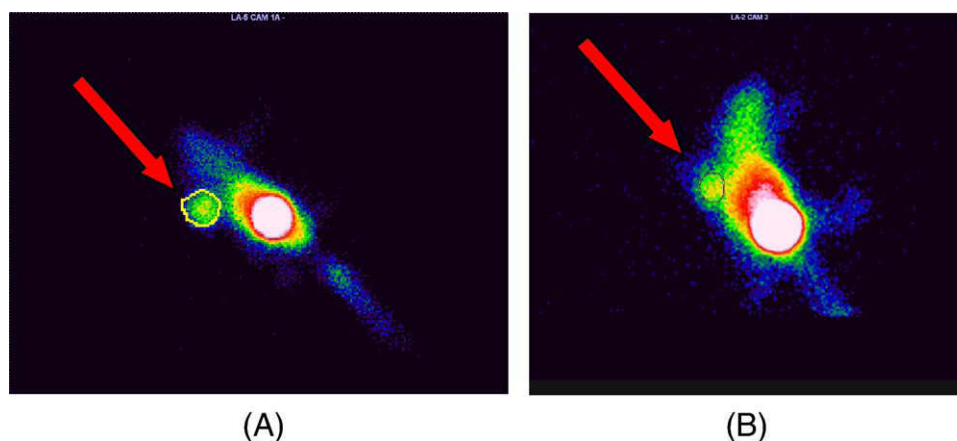| Ratio	^{99m}Tc-HYNIC-BBN		^{99m}TcN(PNP6)-Cys-BBN	
	Unblocked	Blocked	Unblocked	Blocked
Tumor/blood	7.5	3.1	3.1	2.9
Tumor/kidney	0.5	0.3	0.6	0.25
Tumor/liver	2.9	1.7	0.2	0.13
Tumor/muscle	7.0	7.3	2.7	1.5
Tumor/pancreas	0.9	2.4	0.19	0.5
Tumor/intestine	0.7	0.4	0.16	0.09

Fig. 6. Images of mice bearing PC3 tumor xenografts 1.5 h after injection of ^{99m}Tc-HYNIC-BBN: unblocked tumor (A) and blocked tumor with 100 μg of HYNIC-BBN (B).

graphic profile showed one major species with two peaks. Traditionally, these two peaks correspond to syn- and anti-isomers of the same complex, when cysteine is used as chelating group [20]. The heterocomplex is formed by the metal fragment, composed of a terminal Tc≡N multiple bond with an ancillary diphosphine ligand.

The first reaction that occurs under the conditions of this labeling protocol is the reduction of $[^{99m}TcO_4]^-$ by SnCl$_2$ in the presence of succinic dihydrazide [H$_2$N-NH-C(=O)-(CH$_2$)$_2$-(O=)NH-NH$_2$=SDH]. Succinic dihydrazide is the source of nitrido nitrogen groups to yield the Tc≡N bond. In the second phase, the Tc≡N core becomes surrounded by two different bidentate ligands; diphosphine (PNP6) (Fig. 10) and Cys-β-Ala-BBN (Fig. 9), forming a final complex with an asymmetrical structure. The asymmetrical alternative has the advantage of being prepared by simple mixing of PNP and Cys-β-Ala-BBN ligands with the nitrido precursor. The terminal cysteine amino acid residue is able to coordinate the ^{99m}Tc-nitrido phosphine fragment. Cysteine has the appropriate set of pi-donor atoms to

facilitate binding to the $[^{99m}Tc(N)(PNP)]^{2+}$ fragment, generating a bidentate ligand. Therefore, when conjugated to a small peptide such as the BBN analog in Fig. 9, it allows the peptide sequence to remain stable when incorporated into the structure of the final complex.

The use of a spacer group in the molecule can influence clearance of radiopeptide by either the renal-urinary or hepatobilary system, while keeping the metal center and corresponding ligand frameworks some distance away from the active site of the biomolecule, in order to maintain reactivity in vivo. β-Alanine (β-Ala) is a short amino acid spacer containing three carbon atoms which is coupled to the active site of BBN in order to achieve better in vitro and, particularly, in vivo performance.

The length and composition of the spacer group, as well as the physicochemical properties of the radiolabeled moiety, will influence the GRP receptor binding affinity [17]. Garayoa et al. [9] suggested that the ratio of target to nontarget uptake can be improved by insertion of a spacer between the chelator used for labeling and the binding
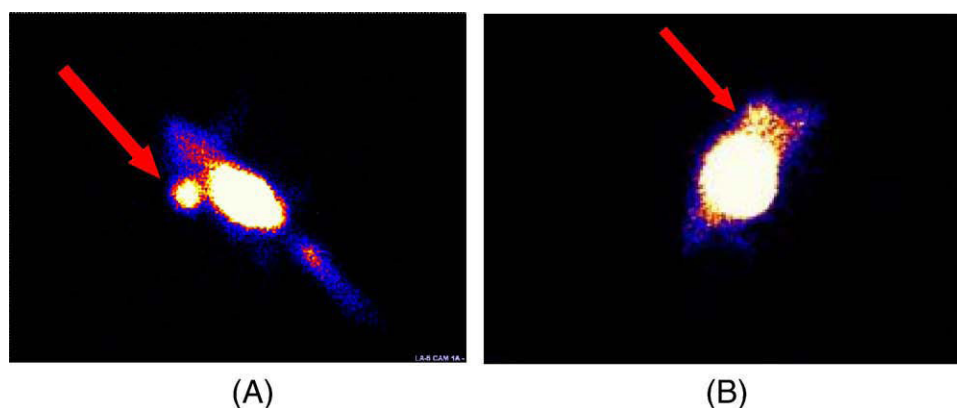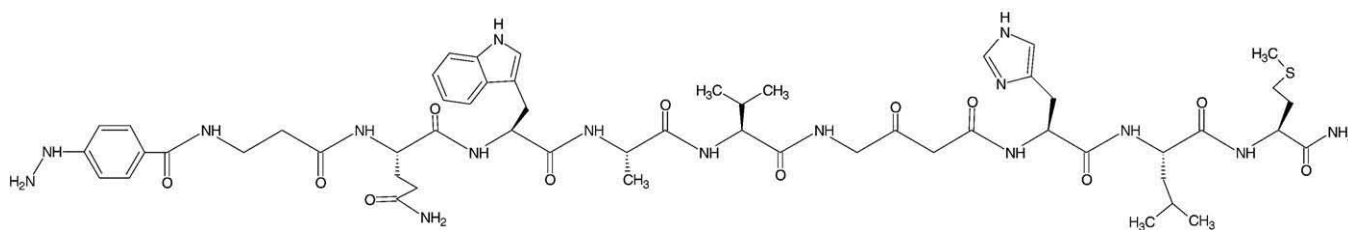

Fig. 7. Images of mice bearing PC3 tumor xenografts 1.5 h after injection of ^{99m}TcN(PNP6)-Cys-BBN: unblocked tumor (A) and blocked tumor with 100 μg of Cys-BBN (B).

Fig. 8. HYNIC-βAla-BBN(7-14)NH$_2$ molecule.

sequence of BBN. Smith et al. [5] investigated the pharmacokinetics and pancreatic accumulation of different analogs with a series of aliphatic spacer groups, and Garayoa et al. [9] used more polar spacers. The former group demonstrated that the carbon length influenced liver uptake in non–tumor-bearing mice and reported that the spacer β-Ala with the derivative N$_3$S-BBN, when labeled with Tc, exhibited the highest uptake in the pancreas when compared to other extension spacers studied. They also registered during biodistribution investigations that, as the hydrocarbon chain length of the spacer group increased, clearance of the radiopeptides by the renal/urinary pathway diminished, with a parallel reduction in pancreatic uptake. Such considerations lend credence to the selection of β-Ala as a spacer in this project.

The pancreas is typically used as an indicator of GRP receptor specificity for BBN conjugates [4,16]. The lipophilic character of the final compound and not the spacer length often dictate the in vivo behavior [4].

As regards the liver, with hydrophobic species, rapid accumulation occurs, in contrast to prompt excretion if the opposite configuration is injected. In both circumstances, there may be less tracer available for a first-pass extraction onto receptor specific tissue. Thus, high uptake by pancreas does not always mean that good tumor binding will occur, as reported by La Bella et al. [26] and Garayoa et al. [9].

La Bella et al. [26] demonstrate high affinity for the GRP receptor of [^{99m}Tc(CO)$_3$-Nα-histidinyl acetate]-BBN(7-14) NH$_2$ in vitro and in vivo; however, minimal concentration in the PC3 tumor followed (0.6$\pm$0.1%ID/g). Tumor uptake achieved in the current study was higher than in studies previously reported [8].

Blocking experiments by coadministration of a known receptor ligand is often used to demonstrate the tumor specificity of a radiotracer. In this study 100 µg/mouse of cold BBN was chosen as the blocking agent. A 50–67% reduction in tumor-specific accumulation of conjugate was observed. Site-directed pancreatic uptake was reduced by $\cong$80%, further demonstrating the effectiveness of these conjugates for targeting the GRP receptor. Coinjection of excess BBN resulted in significant reduction in the uptake of ^{99m}Tc-HYNIC-BBN by liver, pancreas and tumor. In other organs such as lung, kidney, spleen and intestine, a higher radioactivity concentration of conjugate was observed, possibly caused by the saturation effect of BBN in distribution and transport mechanisms.

Both radiotracers showed the same internalization profile with increased values from 30 min to 2 h incubation time. This analogous behaviour was expected as the C-terminal structure of the peptide, related to affinity binding and biological activity, was the same.

Percentage of internalization was moderate, below 20% for both molecules. As values increased with time, it is likely that with longer incubation time, a better outcome would have been reached. Higher values have been reported for certain BBN analogs, but lower figures can also be found [27,28].

It is accepted that in the absence of internalization practical value of the marker becomes questionable. However, actual percentage is not necessarily a reliable index of clinical usefulness, as only after biodistribution studies can the best marker be identified [29].

It has been recently highlighted that GRP receptor agonists may, in some contexts, display an antagonistic performance, and take up by PC3 cells might be influenced
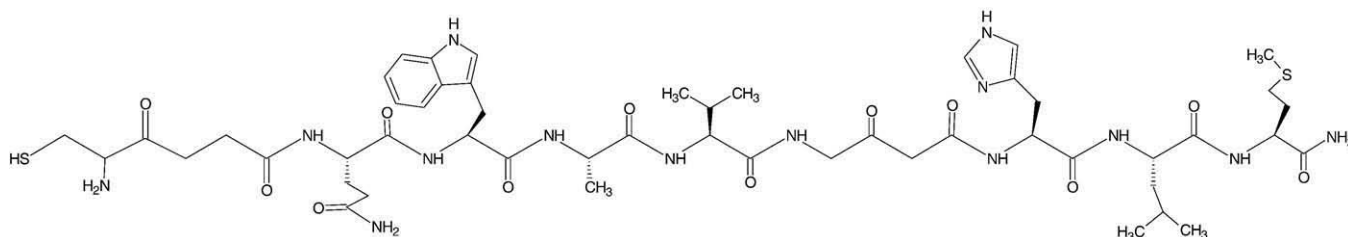
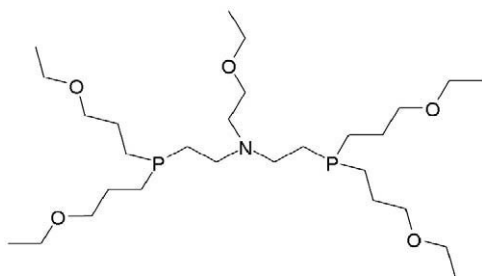Fig. 9. Cys-β-Ala-BBN(7-14)NH$_2$ molecule.

Fig. 10. PNP6 molecule.

by these shifts. Such hypothesis was not investigated in the conditions of this protocol, but it deserves further study [27].

Small discrepancies in the values of some nonspecific organs were also observed, concerning healthy animals and those with tumors. This should be attributed to the different animal models used in the study. Maina et al. [11] called attention to the fact that bombesin-like peptides may have different structure–function relationships in different species, with a given compound functioning as an agonist in one species and as an antagonist in another. Human tumor cells are traditionally inoculated in immunocompromised nude mice for predictable growth without rejection. However, as these are expensive rodents requiring rather cumbersome manipulation, another animal line (Swiss mice) was used as controls.

Good water solubility certainly contributed to the advantageous tumor/tissue and general biodistribution profile of ^{99m}Tc-HYNIC-BBN. By the same token, higher uptake of ^{99m}TcN(PNP6)-Cys-BBN for most organs was very likely due the lipophilicity of this tracer. Indices of tumor accumulation found in invasive studies are consistent with the percentage of ROI obtained in the imaging. Significant accumulation of radioactivity in the abdominal region such as liver and intestine, or even more important for prostate tumors, in the pelvis (urinary bladder), may significantly impair the capacity to effectively distinguish nearby tumors [5]. As previously alluded to, decreasing the lipophilicity of the radiolabeled peptide conjugate serves to increase renal/urinary excretion and decrease residence time in blood, which, for most purposes, is an advantage, but not for prostatic cancer. This problem was not addressed in this exploratory protocol. Yet, it is worth mentioning that several strategies may be available in order to minimize urinary bladder interference. Differential timing of the images in order to highlight the prostate gland before bladder filling is one possibility, whereas bladder drainage by means of an indwelling tube is also an alternative.

5. Conclusion

^{99m}Tc-HYNIC-βAla-BBN and ^{99m}Tc≡N(PNP6)-Cys-βAla-BBN demonstrated high radiochemical yields and good stability. Tumor uptake in tumor-bearing PC3 mouse

models, however, was higher for ^{99m}Tc-HYNIC-BBN. Blocking studies in mice bearing PC3 tumor cells revealed significantly reduced pancreas and tumor uptake, demonstrating the specificity of the complexes for the GRP receptor. In conclusion, ^{99m}Tc-HYNIC-BBN is an ideal radiotracer for targeting GRP receptor-expressing tumors on the basis of high radiochemical yield, fast radiolabeling procedure without need for a purification step and more consistent tumor uptake.

References

[1] Heppeler A, Froidevaux S, Eberle AN, Maecke HR. Receptor targeting for tumor localization and therapy with radiopeptides. Curr Med Chem 2000;7:971–94.

[2] Anastasi A, Erspamer V, Bucci M. Isolation and structure of bombesin and alytesin, two analogous active peptides from the skin of the European amphibians bombesina and alytes. Experientia 1971;27:166–9.

[3] Nagalla SR, Barry BJ, Falick AM, Gibson BW, Tatkir JE, Dong JZ, Spindel ER. There are three distinct forms of bombesin. Identification of [Leu^{13}]bombesin, [Phe^{13}]bombesin, and [Ser^3, Arg^{10}, Phe^{13}] bombesin in the frog *Bombina orientalis*. J Biol Chem 1996;271:7731–7.

[4] Smith CJ, Volkert WA, Hoffman TJ. Gastrin releasing peptide (GRP) receptor targeted radiopharmaceuticals: a concise update. Nucl Med Biol 2003;30:861–8.

[5] Smith CJ, Volkert WA, Hoffman TJ. Radiolabeled peptide conjugates for targeting of the bombesin receptor superfamily subtypes. Nucl Med Biol 2005;32:733–40.

[6] Faintuch BL, Santos RLSR, Souza ALFM, Hoffman TJ, Greeley M, Smith CJ. ^{99m}Tc-HYNIC-bombesin (7-14)NH$_2$: Radiochemical evaluation with co-ligands EDDA (EDDA=ethylenediamine-*N*,*N*′-diacetic acid), tricine, and nicotinic acid. Synth React Inorg Met-Org Nano-Met Chem 2005;35:43–51.

[7] Cornelio DB, Roesler R, Schwartsmann G. Gastrin-releasing peptide receptor as a molecular target in experimental anticancer therapy. Ann Oncol Adv Access 2007. [published March 9 on-line].

[8] Okarvi SM. Peptide-based radiopharmaceuticals: future tools for diagnostic imaging of cancers and other diseases. Med Res Rev 2004; 24:357–97.

[9] Garayoa EG, Ruegg D, Blauenstein P, Zwimpfer M, Kahn IU, Maes V, et al. Chemical and biological characterization of new Re(CO)$_3$/[^{99m}Tc](CO)$_3$ bombesin analogues. Nucl Med Biol 2007;34:17–28.

[10] Hoffman TJ, Quinn TP, Volkert WA. Radiometallated receptor-avid peptide conjugates for specific in vivo targeting of cancer cells. Nucl Med Biol 2001;28:527–39.

[11] Maina T, Nock BA, Zhang H, Nikolopoulou A, Waser B, Reubi JC, et al. Species differences of bombesin analog interactions with GRP-R define the choice of animal models in the development of GRP-R-targeting drugs. J Nucl Med 2005;46:823–30.

[12] Banerjee S, Pillai MRA, Ramamorthy N. Evolution of Tc-99m in diagnostic radiopharmaceuticals. Semin Nucl Med 2001;31:260–77.

[13] Blok D, Feitsma HIJ, Kooy YMC, Welling MM, Ossndorp F, Vermeij P, et al. New chelation strategy allows for quick and clean 99mTc-labeling of synthetic peptides. Nucl Med Biol 2004;31:815.

[14] Van de Wiele C, Dumont F, Broecke RV, Oosterlinck W, Cocquyt V, Serreyn R, et al. Technetium-99m RP527, a GRP analogue for visualization of GRP receptor-expressing malignancies: a feasibility study. Eur J Nucl Med 2000;27:1694–9.

[15] Van de Wiele C, Dumont F, Rudy A, Dierckx RA, Peers SH, Thornback J, et al. Biodistribution and dosimetry of ^{99m}Tc-RP527, a gastrin-releasing peptide (GRP) agonist for the visualization of GRP receptor-expressing malignancies. J Nucl Med 2001;42:1722–7.

[16] Nock B, Nikolopoulou A, Chiotellis E, Loudos G, Maintas D, Reubi JC, et al. [^{99m}Tc]Demobesin 1, a novel potent bombesin analogue for

GRP receptor-targeted tumour imaging. Eur J Nucl Med 2003;30: 247–58.

[17] Karra SR, Schibli R, Gali H, Katti KV, Hoffman TJ, Higginbotham C, Sieckman GL, Volkert WA. ^{99m}Tc labeling and in vivo studies of a bombesin analogue with a novel water-soluble dithiaphosphine-based bifunctional chelating agent. Bioconjug Chem 1999;10: 254–60.

[18] Baldas J, Bonnyman J. Substitution reactions of ^{99m}TcNCl$_4^-$, a new route to a new class of 99mTc-radiopharmaceuticals. Int J Appl Radiat Isot 1985;36:133.

[19] Pasqualini R, Comazzi V, Bellande E, Duatti A, Marchi A. A new efficient method for the preparation of ^{99m}Tc-radiopharmaceuticals containing the Tc≡N multiple bond, Int. Appl Radiat Isot 1992;43: 1329.

[20] Bolzati C, Mahmood A, Malago E, Uccelli L, Boschi A, Jones AG, et al, Duatti A, Tisato F. The $[^{99m}$Tc(N)(PNP)$]^{+2}$ metal fragment: a technetium-nitrido synthon for use with biologically active molecules. The *N*-(2-methoxyphenyl)piperazil-cysteine analogues as examples. Bioconjug Chem 2003;14:1231.

[21] Zhang J, Wang X, Li CY. Synthesis and biodistribution of a new ^{99m}Tc nitrido complex for cerebral imaging. Nucl Med Biol 2002; 29:665.

[22] Zinn KR, Smith CA, Wu Q, Kirkman RL, Mountz JM, Buchsbaum DJ, et al. Imaging adenoviral-mediated gene transfer of gastrin releasing peptide receptor (GRPr) using a Tc-99m-labeled bombesin (BBN) analogue. J Nucl Med 1998;39:224P. [Abstract 994].

[23] www.cancer.org – accessed April 30, 2007.

[24] Markwalder R, Reubi JC. Gastrin-releasing peptide receptors in the human prostate: relation to neoplastic transformation. Cancer Res 1999;59:1152–9.

[25] Liu S, Edwards DS. ^{99m}Tc-labeled small peptides as diagnostic radiopharmaceuticals. Chem Rev 1999;99:2235.

[26] La bella R, Garayoa EG, Langer M, Blauenstein P, Beck-Sickinger AG, Schubiger PA. *In vitro* and *in vivo* evaluation of a ^{99m}Tc(I)-labeled bombesin analogue for imaging of gastrin releasing peptide receptor-positive tumors. Nucl Med Biol 2002;29:553–60.

[27] Cescato R, Maina T, Nock B, Nikolopoulou A, Charalambidis D, Piccand V, et al. Bombesin receptor antagonists may be preferable to agonists for tumor targeting. J Nucl Med 2008;49:318–26.

[28] Kunstler JU, Veerendra B, Figueroa SD, Sieckman GL, Rold TL, Hoffman TJ, et al. Organometallic 99mTc(III)′4 + 1′ bombesin(7-14) conjugates: synthesis, radiolabeling, and in vitro/in vivo studies. Bioconjug Chem 2007;18:1651–61.

[29] Smith CJ, Gali H, Sieckman GL, Higginbotham C, Volkert WA, Hoffman TJ. Radiochemical investigations of 99mTc-N3S-X-BBN [7-14]NH2: an in vitro/in vivo structure-activity relationship study where X) 0-, 3-, 5-, 8-, and 11-carbon tethering moieties. Bioconjug Chem 2003;14:93–102.